Transactions of the Nigerian Association of Mathematical Physics
Volume 15, (April –June, 2021 Issue), **pp19 – 28**

NUMERICAL SOLUTION FOR THE PIPE DIAMETERS AND WALL THICKNESS OF WATER HAMMER MODEL USING CRANK-NICOLSON ALGORITHM

AYODELE V.I.[1] and FALADE K.I[2]

[1]Department of Computer Science and Mathematics, Faculty of Science, Nigeria Police Academy, Wudil Kano State Nigeria.
[2]Department of Mathematics, Faculty of Computing and Mathematical Sciences, Kano University of Science and Technology, P.M.B 3244 Wudil Kano State Nigeria.

Abstract

Crack-Nicolson algorithm was formulated and applied to solve frictionless water–hammer equation. The system of partial differential equations are important in applied fluid dynamics and thermodynamics study, however are often harder to solve analytically and process on how to solve them has been slow. These drawbacks motivated the use of the proposed approach with short computational time and lower operation count results in reduction of cumulative truncation errors and improvement of overall accuracy. The objective is to vary the inner diameters and wall thickness on water hammer on four (4) pipes test cases with density of water are considered.The numerical solutions obtained are plotted on 2Dplots and 3Dplots to illustrate the efficiency of the proposed algorithm. The advantage of the present algorithm is that it show high performance in evaluation of the solutions and reduction in time taken for solve any system of partial differential equations arises in applied sciences and engineering. Finally, all computational and algorithm works are implemented using MAPLE 18 software version.

Keywords: Crack-Nicolson algorithm, frictionless water–hammer equation, density of water, inner diameters, wall thickness,MAPLE 18 software version.

1.0 INTRODUCTION

Large pipe systems with long pipelines transporting fluids over great distances are reality in modern society. The usage of small pipe diameters, high-velocity together with sophisticated fluid control devices, many types of pumps and valves, coupled with electronic sensors have increased the importance of correct design. Nuclear power plants have systems with large networks of piping both for the production of electricity and to ensure water cooling at all times in a reliable and safe way. The water in nuclear power plants is often under high pressure and at high flow rate generated by pumps. Pump failure, improper operations of valves and accidental events like power losses and pipe ruptures create transient flows, which can lead to pressure waves through the pipe system. A sudden change in flow like that generates a pressure pulse. This phenomenon is called water hammer.

The waterhammer means that the dynamic loads are induced on the pipe, the pipe support and the equipment in the system due to the sudden change of the flow velocity inside the pipe. The sudden changes are mainly caused by the valve sudden on/off and pump sudden start/trip. Waterhammer can occur in any thermal-hydraulic systems. Waterhammer can reach pressure levels far exceeding the pressure range of a pipe given by the manufacturer, and it can lead to the failure of the pipeline integrity. In the past three decades, since a large number of waterhammer events occurred in the light-water-reactor power plants, a number of comprehensive studies on the phenomena associated with waterhammer events have been performed. There are three basic types of severe waterhammer occurring at power plants that can result in significant plant damage: rapid valve operation events; void-induced waterhammer; condensation-induced waterhammer. Correct prediction of waterhammer transients, is therefore of paramount importance for the safe operation of the plant. Therefore verifying of computer codes capability to simulate waterhammer type transients is very important issue at performing of

Correspondence Author: Ayodele V.I., Email: dunniayodele@yahoo.com, Tel: +2348068713169

safety analyses for nuclear power plants [1]. This phenomena can endanger the integrity of structures leading to a possible failure of pipes in nuclear power plants as well as in many industrial applications. These phenomena can arise in nuclear power plants in the course of transients and accidents induced by the start-up of auxiliary feed water systems or emergency core cooling systems in combination with rapid acting valves and pumps [2]. Moreover, Waterhammer can occur in any thermal-hydraulic systems. Waterhammer can reach pressure levels far exceeding the pressure range of a pipe given by the manufacturer, and it can lead to the failure of the pipeline integrity. In the past three decades, since a large number of waterhammer events occurred in the light-water- reactor power plants, a number of comprehensive studies on the phenomena associated with waterhammer events have been performed. There are three basic types of severe waterhammer occurring at power plants that can result in significant plant damage: rapid valve operation events; void-induced waterhammer; condensation-induced waterhammer. Correct prediction of waterhammer transients, is therefore of paramount importance for the safe operation of the plant. Therefore verifying of computer codes capability to simulate waterhammer type transients is very important issue at performing of safety analyses for nuclear power plants [3]. Many examples are given of solution of water hammer of common pipe-line systems as well as calculation of the steady state of flow, the determination of discharge through a pipe-line, measurements of characteristics of valves, pumps, turbines, determination of the operating régime of a valve in order to ensure a desired pressure and discharge curve which are core interest in those civil, mechanical and petroleum engineers dealing with the design and operation of hydraulic systems [4].

2.0 WATER HAMMER MODEL

When a valve at the end of a pipeline suddenly closes, a pressure surge hits the valve and travels along the pipeline. This is known as water hammer phenomenon. This process is modeled by system partial differential equations (SPDEs) which represent the fundamental conservation equations of classic frictionless water–hammer equationof the form [6].

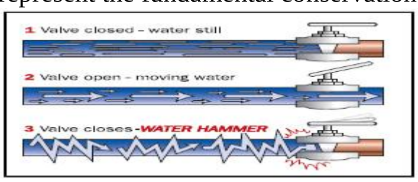

Figure.1 Water Hammer Description [5]

$$\begin{cases} \frac{\partial V}{\partial t} + \frac{1}{\rho_f}\frac{\partial P}{\partial z} = 0 & (1) \\ \frac{\partial V}{\partial z} + \frac{1}{\rho_f a_h}\frac{\partial P}{\partial t} = 0 & (2) \end{cases}$$

Where equations (1) and (2) are continuity and momentum (dynamics) equations, $V$and P are instantaneous fluid velocity (m/s) and transient pressure in temporal dimension (Pa) respectively, ρ_f is fluid density and $a_h$wave speed in fluids define as

$$a_h = \sqrt{\frac{K}{\rho_f\left(1 + \frac{DK}{eE}\right)}} \qquad (3)$$

Here, K is bulk modulus of compressibility,ρ_f is fluid density, D is pipe inner diameter and e pipe-wall thickness.

Couple with initial and boundary conditions

$$\begin{cases} V(0,t) = g(t) \\ P(0,t) = h(t) \end{cases} \qquad (4)$$

$$\begin{cases} V(L,t) = g(t)^* \\ P(L,t) = h(t)^* \end{cases} \qquad (5)$$

$$\begin{cases} V(z,t) = g(z) \\ P(z,t) = h(z) \end{cases} \qquad (6)$$

In this paper, we consider the following assumptions:

i. One dimensional flow equations of water hammer.
ii. The pipe is water (Turbulent state) and remains at this condition during the transients.
iii. The behavior of both, the liquid and the pipe-wall is linearly elastic.
iv. Horizontal pipe-slope, subject to variation of diameters and lengths.
v. There is neither vacuum nor bubbles generation nor separation of column.

Water hammer phenomenon is basically mean a transient that begins when the steady state flow conditions in a confined fluid are partial perturbed with parameters such as inner diameter and wall thickness. The study of this situation have received less attention than the typical ones in fluid dynamics. However, fluid velocity is conditioned since the conduit are by pipe diameter and wall thickness as expressed in the mass balance formulation and fluid velocity shows continuous changes during water hammer, therefore pipe diameter and wall thickness must have directs incidence respect to this phenomena [7].

Classical water–hammer theory is also based on this principle. Since then, many researchers have added their contributions in a step-wise manner, building up and shaping the theory of hydraulic transients in pipe flow in last four decades. Various researchers worked on numerical solution and analysis of this model such as [8] formulated a model of the water Hammer effect considering a spring safety valve which he considers a method for calculating the water Hammer effect in a hydraulic system with a string safety valve. The developed model enables simulation testing in order to estimate the influence of construction parameters of the string activated safety valve on pressures changes and on the velocity of fluid flow along the pipe. Author [1] analyze the inner diameter influence on water hammer phenomena and also formulation of analytical algorithm for solving the unsteady-one- dimensional water hammer model was carried out and it allowed estimating the instantaneous head at any point of a single pipeline. The model was solved by mean of Laplace's transformed. To determine the influence of internal- diameter conduit on the pressure oscillation, four distinct inside-diameter values were introduced into the solution.it was founded that the wave frequency is sensitive to the variation of the pipe-diameter. The author in [9] presented a different ways of water- hammer computation and the procedure is based on the method of characteristics but a numerical grid is not required. The computation was based on back-tracking waves by means of a very simple recursion, so that the programming effort is small. Exact solutions are thus obtained for frictionless water-hammer and approximate solutions are obtained when the distributed friction in individual's pipes is concentrated at the pipe boundaries. The influence of pipe-Diameter on water Hammer phenomena was discussed in [7], the authors in [10] further investigated water hammer model with experimental results are obtained. They considered four different configurations of steel and a plastic pipeline. Extremely high pressure peaks were recorded immediately upon collapse of the vapour cavity. The pressure then dropped to about 40% of the pressure peak level and maintained this level for twice of a second. Authors [11] studied one-dimensional fluid–structure interaction models in pressurized fluid-filled pipes. The fluid contained a minimal amount of dissolved gas and emphasized on limited cavitation while experimental results showed that the maximum pressure may exceed the Joukowsky pressure rise in the form of short duration pressure pulse. They observed that the reservoir pressure was rising during the experiment because the tank was too small.

3.0 CRANK-NICOLSON METHOD (CNM)

Crank Nicolson method is one of the numerical methods to solve a partial differential equation the most successful difference method for parabolic equations is due to John Crank and Phyllis Nicolson (1947). Crank Nicolson method is a finite difference method used for solving heat equation and similar partial differential equations. This method is of order two in space, implicit in time, unconditionally stable and has higher order of accuracy. It is based on a convex combination of the spatial terms of the forward and backward difference methods. Crank Nicolson Method for solving parabolic partial differential equations was developed by John Crank and Phyllis Nicolson in the mid-20th century. A practical method for numerical evaluation of partial differential equations of the heat conduction type was considered by [12], Authors [13] applied Crank Nicolson method parabolic partial differential equations, and Author [14] presented numerical solution of parabolic initial – boundary value problem with Crank-Nicolson's finite difference equations. Moreover, the modification of explicit scheme and proved that it is much more stable than the simple explicit case, enabling larger time steps to be used and considered the stability and accuracy of finite difference method for option pricing. However, the accuracy of the simple explicit method is barely improved upon [15, 16].

Consider finite difference approximation derivatives of velocity v and pressure p by Taylors formular

$$\begin{cases} v(t+h,z) = v(t,z) + h\dfrac{\partial v}{\partial t} + \dfrac{1}{2!}h^2\dfrac{\partial^2 v}{\partial t^2} + \dfrac{1}{3!}h^3\dfrac{\partial^3 v}{\partial t^3} + \cdots \\ p(t+h,z) = p(t,z) + h\dfrac{\partial p}{\partial t} + \dfrac{1}{2!}h^2\dfrac{\partial^2 p}{\partial t^2} + \dfrac{1}{3!}h^3\dfrac{\partial^3 p}{\partial t^3} + \cdots \end{cases} \quad (7)$$

$$\begin{cases} v(t-h,z) = v(t,z) - h\dfrac{\partial v}{\partial t} + \dfrac{1}{2!}h^2\dfrac{\partial^2 v}{\partial t^2} - \dfrac{1}{3!}h^3\dfrac{\partial^3 v}{\partial t^3} + \cdots \\ p(t-h,z) = p(t,z) - h\dfrac{\partial p}{\partial t} + \dfrac{1}{2!}h^2\dfrac{\partial^2 p}{\partial t^2} - \dfrac{1}{3!}h^3\dfrac{\partial^3 p}{\partial t^3} + \cdots \end{cases} \quad (8)$$

From (7) neglecting $h^2$and higher power of h we obtain forward difference

$$\begin{cases}\frac{\partial v}{\partial t}\approx\frac{v(t+h,z)-v(t,z)}{h}\\ \frac{\partial p}{\partial t}\approx\frac{p(t+h,z)-p(t,z)}{h}\end{cases}\qquad(9)$$

From (8) neglecting $h^2$and higher power of h we obtain backward difference

$$\begin{cases}\frac{\partial v}{\partial t}\approx\frac{v(t,z)-v(t-h,z)}{h}\\ \frac{\partial p}{\partial t}\approx\frac{p(t,z)-p(t-h,z)}{h}\end{cases}\qquad(10)$$

Subtracting (8) from (7) and neglecting $h^2$and higher power of h we obtain central difference

$$\begin{cases}\frac{\partial v}{\partial t}=\frac{1}{2h}\big(v(t+h,z)-v(t-h,z)\big)\\ \frac{\partial p}{\partial t}=\frac{1}{2h}\big(p(t+h,z)-p(t-h,z)\big)\end{cases}(11)$$

Similarly,

$$\begin{cases}\frac{\partial v}{\partial z}\approx\frac{v(t,z+k)-v(t,z)}{k}\\ \frac{\partial p}{\partial z}\approx\frac{p(t,z+k)-p(t,z)}{k}\end{cases}\qquad(12)$$

$$\begin{cases}\frac{\partial v}{\partial t}\approx\frac{v(t,z)-v(t,z-k)}{k}\\ \frac{\partial p}{\partial t}\approx\frac{p(t,z)-p(t,z-k)}{k}\end{cases}\qquad(13)$$

$$\begin{cases}\frac{\partial v}{\partial z}\approx\frac{v(t,z+k)-v(t,z-k)}{2k}\\ \frac{\partial p}{\partial z}\approx\frac{p(t,z+k)-p(t,z-k)}{2k}\end{cases}\qquad(14)$$

In order to obtain Crack Nicolson scheme for classic frictionless water–hammer equation (1) and (2), we substitute and discretizing equations (9) to (14) as follow:

$$\begin{cases}\frac{\partial v}{\partial z}\approx\frac{1}{4h}(v[i+1,j+1]-v[i-1,j+1]+v[i+1,j]-v[i-1,j])\\ \frac{\partial p}{\partial z}\approx\frac{1}{4h}(p[i+1,j+1]-p[i-1,j+1]+p[i+1,j]-p[i-1,j])\\ \frac{\partial v}{\partial t}\approx\frac{1}{k}(v[i,j+1]-v[i,j])\\ \frac{\partial p}{\partial t}\approx\frac{1}{k}(p[i,j+1]-p[i,j])\end{cases}\qquad(15)$$

$$\begin{cases}\frac{1}{k}(v[i,j+1]-v[i,j])+\frac{1}{\rho_f}\frac{1}{4h}(p[i+1,j+1]-p[i-1,j+1]+p[i+1,j]-p[i-1,j])\\ \frac{1}{4h}(v[i+1,j+1]-v[i-1,j+1]+v[i+1,j]-v[i-1,j])+\frac{1}{\rho_f a_h}\frac{1}{k}(p[i,j+1]-p[i,j])\end{cases}\qquad(16)$$

Equation (16) is called the Crank Nicolson approximation for numerical solution of water hammer equation and its associated with boundary and initial conditions given in (4) to (6) which be arranged with step $(i+1)$ and $(j+1)$ of the equations to all the nodes to form tridiagonal coefficient matrix at $i=1,2,..h-1$ and $j=1,2,..k-1$.

In order to reduce the time taken in computational and evaluation to execute crack- Nicolson scheme, we formulate a seven steps algorithm using MAPLE 18 software package as follow:

restart:
with(PDEtools):
Step 1:
$Digits := 15;$
$[\rho[\mathrm{f}], K, d, e, E \in \mathbb{R}^+]$

$$a[h] := \sqrt{\frac{K}{\rho[\mathrm{f}] * \left(1+\frac{d*K}{e*E}\right)}};$$

Step 2:
$V[z] := \frac{1}{4*h} * (v[i+1,j+1] - v[i-1,j+1] + v[i+1,j] - v[i-1,j]);$
$P[z] := \frac{1}{4*h} * (p[i+1,j+1] - p[i-1,j+1] + p[i+1,j] - p[i-1,j]);$
$V[t] := \frac{1}{k} * (v[i,j+1] - v[i,j]);$
$P[t] := \frac{1}{k} * (p[i,j+1] - p[i,j]);$
Step 3:
$V[i,j] = v[t] + \frac{1}{\rho[f]} * \rho[f];$
$B[i,j] = v[z] + \frac{1}{\rho[f] * a[h]} * P[t];$
$h := \mathbb{R}^+;$
$k = \mathbb{R}^+;$
$N := \mathbb{R}^+$
Step 4:
$for t\ from\ 1\ to\ N\ do\ [0,t] = 100 * t^2;$ p $[0,t] = 2 * t; end\ do$:
$for t\ from\ 0\ to\ N\ do\ v\ [10,t] = t^2;$ p $[10,t] = t + 1; end\ do$:
$for z\ from\ 0\ to\ 9\ do\ v\ [z,0] = z^2 + 1;$ p $[z,0] = z + 1; end\ do$:
Step 5:
$for i\ from\ 1\ to\ 9\ do$
$for j\ from\ 0\ to\ N\ do$
$A[i,j] = \frac{(v[i,j+1]-v[i,j])}{k} + \frac{1}{4} * \left(\frac{1}{\rho[f]}\right) \frac{(p[i+1,j+1]-p[i-1,j+1]+p[i+1,j]-p[i-1,j])}{h}$

$B[i,j] = \frac{1}{4} \frac{(v[i+1,j+1]-v[i-1,j+1]+v[i+1,j]-v[i-1,j])}{h} + \left(\frac{1}{\rho[f]*a[h]}\right) * \frac{(p[i,j+1]-p[i,j])}{k}$
$end\ do$
Step 6:
$P[sol] = seq * (seq(A[m,n], m = (1 \ldots 9), n = 0 \ldots N-1)$:
$V[sol] = seq * (seq(B[m,n], m = (1 \ldots 9), n = 0 \ldots N-1)$:
$R = \{P, V\}$:
$solve(R)$
Step 7:
$\mathrm{2Dplot[1]} := \mathrm{plot}([\mathrm{V[sol]}]), \mathrm{t} = 0 \ldots 10, \mathrm{color} = [\mathrm{blue}], \mathrm{axes} = \mathrm{BOXED}, \mathrm{title} = \mathrm{cases});$
$\mathrm{2Dplot[2]} := \mathrm{plot}([\mathrm{P[sol]}]), \mathrm{t} = 0 \ldots 10, \mathrm{color} = [\mathrm{red}], \mathrm{axes} = \mathrm{BOXED}, \mathrm{title} = \mathrm{cases});$
$[\mathrm{3Dplot}] := \mathrm{plot3d}([\mathrm{P,V}], \mathrm{t} = 0 \ldots 1, \mathrm{z} = 0 \ldots 1, \mathrm{grid} = [100{,}100], \mathrm{blue}, \mathrm{red});$
Output: See
Tables (3,4,5,6) and plots (1,2,3,…,12).
Where $\mathbb{R}^+$ Set of positive integers.

3.0 NUMERICAL IMPLEMENTATION

In this section, numerical experiment was carried out to illustrate the efficiency of the proposed algorithm. We considered four test pipe cases to examine the effect of density of fluid ρf, pipe diameters D and wall thickness e on a system of frictionless partial differential equations (1) and (2). Considering parameters given in Table 1 and nodal point of $N = 4$ with $h = k = 0.5$. Subsequently we applied CNA formulated (17) to obtain numerical solutions for instantaneous fluid velocity (m/s) and transient pressure in temporal dimension $(Pa)$of frictionless water–hammer equations.

Table 1. Experimental Parameters (pipe diameter and wall thickness)

Parameters	Pipe 1 (water)	Pipe 2 (water)	Pipe 3 (water)	Pipe 4 (water)
Liquid density ρf	$\rho = 1.0g/ml$	$\rho = 1.0g/ml$	$\rho = 1.0g/ml$	$\rho = 1.0g/ml$
Bulk modulus K	$k = 200E10^6$	$k = 200E10^6$	$k = 200E10^6$	$k = 200E10^6$
Pipe diameter D	$1000mm$	$2000mm$	$3000mm$	$4000mm$
Wall thickness e	$20mm$	$30mm$	$40mm$	$50mm$
Young's modulus E	$E = 70E10^9$	$E = 70E10^9$	$E = 70E10^9$	$E = 70E10^9$
Initial condition $g(t)$	$100t^2$	$100t^2$	$100t^2$	$100t^2$
Initial condition $h(t)$	$2t$	$2t$	$2t$	$2t$
Boundary condition $g(t)^*$	t^2	t^2	t^2	t^2
Boundary condition $h(t)^*$	$t+1$	$t+1$	$t+1$	$t+1$
Boundary condition $g(z)$	z^2+1	z^2+1	z^2+1	z^2+1
Boundary condition $h(z)$	$z+1$	$z+1$	$z+1$	$z+1$

Table 2. Grid lines with nodal points $N = 4$

0, 4 V,P (600,9)	1,4	2,4	3,4	4,4	5,4	6,4	7,4	8,4	9,4	10, 4 V,P (9,4)
0, 3 V,P (400,4)	1,3	2,3	3,3	4,3	5,3	6,3	7,3	8,3	9,3	10, 3 V,P (4,3)
0, 2 V,P (100,2)	1,2	2,2	3,2	4,2	5,2	6,2	7,2	8,2	9,2	10, 2 V,P (1,2)
0, 1	1,1	2,1	3,1	4,1	5,1	6,1	7,1	8,1	9,1	10, 1 V,P (0,1)
0,0	1,0	2,0	3,0	4,0	5,0	6,0	7,0	8,0	9,0	
V,P → (1,1)	(2,2)	(5,3)	(10,4)	(17,5)	(26,6)	(37,7)	(50,8)	(65,9)	(82,10)	

4.1 NUMERICAL SOLUTIONS FOR INSTANTANEOUS FLUID VELOCITY (m/s) AND TRANSIENT PRESSURE IN TEMPORAL DIMENSION (Pa)

Table 3. Case 1. Pipe diameter $D = 1000mm$ and Wall thickness $e = 20mm$

$V_{i,j}, P_{i,j}$	$t = 0.5$	$t = 1.0$	$t = 1.5$	$t = 2.0$
$V_1(0.5)$	1.25007441176678	1.25029174147269	2.25063191030195	4.25105712359293
$P_1(0.5)$	2.00173862621879	2.01105536289034	2.03552817725729	2.08271585201307
$V_2(1.0)$	4.00054804366449	3.00408668439208	2.01629937978058	1.04665359596992
$P_2(1.0)$	2.99970235293286	2.99942832824351	2.99921099643944	2.99908815039667
$V_3(1.5)$	9.00007677401684	8.00031300161159	7.00072876132661	6.00136184693086
$P_3(1.5)$	3.99954645156083	3.99909297463794	3.99863978395571	3.99818738055730
$V_4(2.0)$	16.0000755951267	15.0003023983855	14.0006804992140	13.0012101659868
$P_4(2.0)$	4.99939525686550	4.99879051393188	4.99818577189097	4.99758103252816
$V_5(2.5)$	25.0000755930062	24.0003023726999	23.0006803418095	22.0012095068064
$P_5(2.5)$	5.99924407105411	5.99848814210940	5.99773221317040	5.99697628425104
$V_6(3.0)$	36.0000755884304	35.0003023359992	34.0006801900320	33.0012090642924
$P_6(3.0)$	6.99909288484071	6.99818576718178	6.99727864220289	6.99637150222832
$V_7(3.5)$	49.0000980324314	48.0004346417113	47.0010901164968	46.0021352726752
$P_7(3.5)$	7.99894171733247	7.99788350555584	7.99682543359282	7.99576756678706
$V_8(4.0)$	63.9991306902834	62.9965511424861	61.9923370505702	60.9866019692225
$P_8(4.0)$	8.99870075511502	8.99723145978798	8.99561105045481	8.99385846926278
$V_9(4.5)$	85.7496751887788	88.9986582425045	91.7468688700652	93.9942362499946
$P_9(4.5)$	10.0024189561988	10.0047244578785	10.0068408489340	10.0086924768366

Table 4. **Case 2. Pipe diameter $D = 2000mm$ and Wall thickness $e = 30mm$**

$V_{i,j}$,$P_{i,j}$	$t = 0.5$	$t = 1.0$	$t = 1.5$	$t = 2.0$
$V_1(0.5)$	1.25007594619169	1.25029775739676	2.25064494077121	4.25107892233760
$P_1(0.5)$	2.00177447773597	2.01128333043978	2.03626078390213	2.08442147773953
$V_2(1.0)$	4.00055934462135	3.00417095360333	2.01663547771173	1.04761559766653
$P_2(1.0)$	2.99969621523326	2.99941653994643	2.99919472655577	2.99906934717868
$V_3(1.5)$	9.00007835715246	8.00031945592753	7.00074378888442	6.00138992907068
$P_3(1.5)$	3.99953709925058	3.99907427299724	3.99861174491106	3.99815003691138
$V_4(2.0)$	16.0000771540001	15.0003086346240	14.0006945350357	13.0012351347919
$P_4(2.0)$	4.99938278662340	4.99876557345604	4.99814836121859	4.99753115177081
$V_5(2.5)$	25.0000771517912	24.0003086078682	23.0006943710728	22.0012344481463
$P_5(2.5)$	5.99922848325031	5.99845696650189	5.99768544975954	5.99691393303808
$V_6(3.0)$	36.0000771470248	35.0003085696383	34.0006942129714	33.0012339871949
$P_6(3.0)$	6.99907417945850	6.99814835631320	6.99722252554299	6.99629667915236
$V_7(3.5)$	49.0001000538871	48.0004436039721	47.0011125939167	46.0021792987795
$P_7(3.5)$	7.99891989515119	7.99783986414702	7.99675997878187	7.99568030712174
$V_8(4.0)$	63.9991127646662	62.9964800259772	61.9921790408866	60.9863257091409
$P_8(4.0)$	8.99867396391023	8.99717437152129	8.99552055055637	8.99373183468788
$V_9(4.5)$	85.7496684909776	88.9986305748354	91.7468043053549	93.9941174016659
$P_9(4.5)$	10.0024688364865	10.0048218775675	10.0069819057240	10.0088717071624

Table 5. **Case 3. Pipe diameter $D = 3000mm$ and Wall thickness $e = 40mm$**

$V_{i,j}$,$P_{i,j}$	$t = 0.5$	$t = 1.0$	$t = 1.5$	$t = 2.0$
$V_1(0.5)$	1.25007670189391	1.25030072023142	2.25065135826031	4.25108965819172
$P_1(0.5)$	2.00179213455733	2.01139560412447	2.03662159155063	2.08526149562151
$V_2(1.0)$	4.00056491032609	3.00421245606031	2.01680100539077	1.04808938178885
$P_2(1.0)$	2.99969319242434	2.99941073422562	2.99918671365882	2.99906008661557
$V_3(1.5)$	9.00007913684465	8.00032263466949	7.00075118993624	6.00140375948527
$P_3(1.5)$	3.99953249325297	3.99906506249195	3.99859793586132	3.99813164571852
$V_4(2.0)$	16.0000779217438	15.0003117059715	14.0007014477102	13.0012474321075
$P_4(2.0)$	4.99937664504573	4.99875329030489	4.99812993651256	4.99750658556569
$V_5(2.5)$	25.0000779194908	24.0003116786806	23.0007012804681	22.0012467317294
$P_5(2.5)$	5.99922080627767	5.99844161255663	5.99766241884184	5.99688322514857
$V_6(3.0)$	36.0000779146291	35.0003116396861	34.0007011192049	33.0012462615595
$P_6(3.0)$	6.99906496708248	6.99812993150908	6.99719488815828	6.99625982887471
$V_7(3.5)$	49.0001010494506	48.0004480178682	47.0011236639929	46.0022009815067
$P_7(3.5)$	7.99890914776147	7.99781837084446	7.99672774247916	7.99563733209276
$V_8(4.0)$	63.9991039363262	62.9964450012124	61.9921012214149	60.9861896516707
$P_8(4.0)$	8.99866076927992	8.99714625564123	8.99547597952747	8.99366946745040
$V_9(4.5)$	85.7496651923200	88.9986169485503	91.7467725073424	93.9940588690869
$P_9(4.5)$	10.0024934024567	10.0048698566043	10.0070513759094	10.0089599776391

Table 6. **Case 4. Pipe diameter $D = 4000mm$ and Wall thickness $e = 50mm$**

$V_{i,j}$,$P_{i,j}$	$t = 0.5$	$t = 1.0$	$t = 1.5$	$t = 2.0$
$V_1(0.5)$	1.25007715176232	1.25030248400248	2.25065517858207	4.25109604923003
$P_1(0.5)$	2.00180264563566	2.01146244047147	2.03683637975687	2.08576155684657
$V_2(1.0)$	4.00056822358132	3.00423716240533	2.01689954373740	1.04837142463177
$P_2(1.0)$	2.99969139295071	2.99940727808866	2.99918194359298	2.99905457381519
$V_3(1.5)$	9.00007960099424	8.00032452696980	7.00075559577117	6.00141199270977
$P_3(1.5)$	3.99952975131038	3.99905957950070	3.99858971539935	3.99812069762663
$V_4(2.0)$	16.0000783787808	15.0003135343427	14.0007055628310	13.0012547527478
$P_4(2.0)$	4.99937298897374	4.99874597816341	4.99811896831275	4.99749196134102
$V_5(2.5)$	25.0000783765013	24.0003135067308	23.0007053936214	22.0012540441302
$P_5(2.5)$	5.99921623618731	5.99843247237595	5.99764870857096	5.99686494478785
$V_6(3.0)$	36.0000783715823	35.0003134672775	34.0007052304609	33.0012535684289
$P_6(3.0)$	6.99905948296873	6.99811896325037	6.99717843566312	6.99623789195569
$V_7(3.5)$	49.0001016421079	48.0004506454522	47.0011302539853	46.0022138891794
$P_7(3.5)$	7.99890274985822	7.99780557592406	7.99670855228923	7.99561174919761
$V_8(4.0)$	63.9990986808294	62.9964241510290	61.9920548956272	60.9861086569416
$P_8(4.0)$	8.99865291453704	8.99712951830476	8.99544944647661	8.99363234036562
$V_9(4.5)$	85.7496632286343	88.9986088368447	91.7467535780401	93.9940240247506
$P_9(4.5)$	10.0025080265405	10.0048984184435	10.0070927313768	10.0090125248527

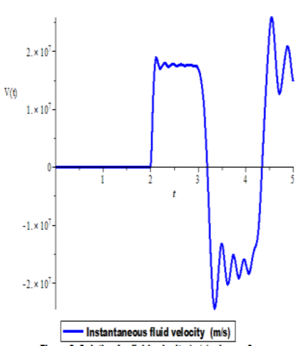

Figure 2. Solution for fluid velocity (m/s) when z=0 Diameter 1000mm and wall thickness 20mm case 1

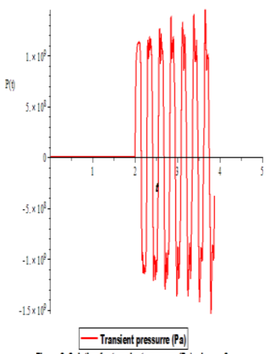

Figure 3. Solution for transient pressure (Pa) when z=0 Diameter 1000mm and wall thickness 20mm case 1

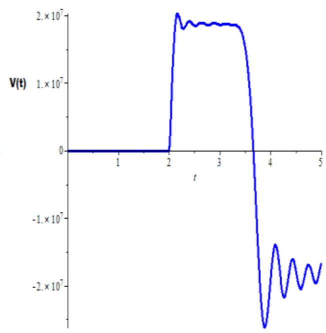
Figure 4. Solution for fluid velocity (m/s) when z=0 Diameter 2000mm and wall thickness 30mm case 2

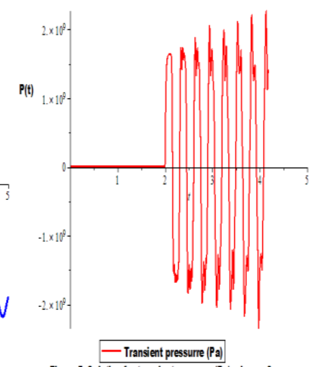

Figure 5. Solution for transient pressure (Pa) when z=0 Diameter 2000mm and wall thickness 30mm case 2

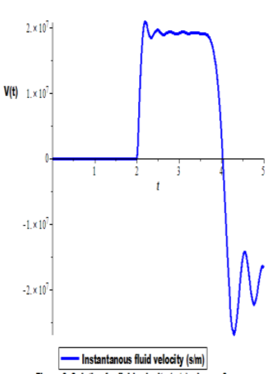

Figure 6. Solution for fluid velocity (m/s) when z=0 Diameter 3000mm and wall thickness 40mm case 3

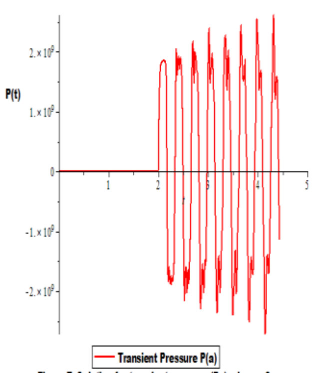

Figure 7. Solution for transient pressure (Pa) when z=0 Diameter 3000mm and wall thickness 40mm case 3

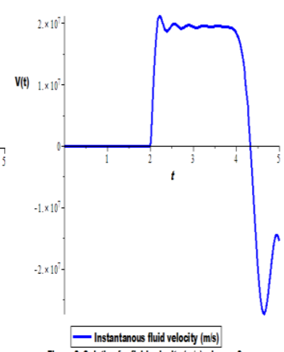

Figure 8. Solution for fluid velocity (m/s) when z=0 Diameter 4000mm and wall thickness 50mm case 4

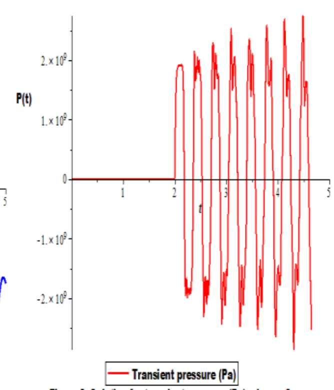

Figure 9. Solution for transient pressure (Pa) when z=0 Diameter 4000mm and wall thickness 50mm case 4

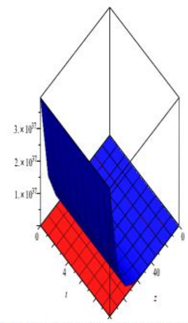

Figure 10. Solution for Fluid velocity (m/s) (blue) vs transient pressure P(a) (red) Diameter 1000mm and wall thickness 20mm case 1

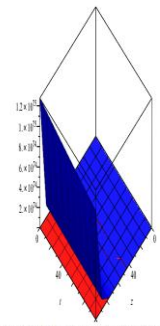

Figure 11. Solution for Fluid velocity (m/s) (blue) vs transient pressure P(a) (red) Diameter 2000mm and wall thickness 30mm case 2

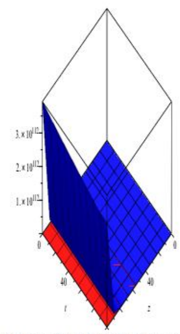

Figure 12. Solution for Fluid velocity (m/s) (blue) vs transient pressure P(a) (red) Diameter 3000mm and wall thickness 40mm case 3

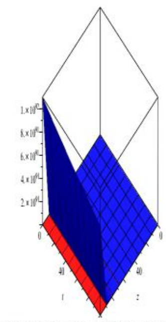

Figure 13. Solution for Fluid velocity (m/s) (blue) vs transient pressure P(a) (red) Diameter 4000mm and wall thickness 50mm case 4

5.0 DISCUSSION AND CONCLUSION

5.1 Discussion

In this paper, we formulate seven steps Crack-Nichoson algorithm for the numerical solutions of one dimension classic frictionless water–hammer equation for density of water was considered. The variation in diameter and pipe wall thickness are examine and numerical solutions are obtained. From the results obtained we observe the following:

i. The flow pertain for instantaneous velocity and transient pressure for equations (1) to (6) are under intermediate influence of diameter and wall thickness (Figures 2 to 9).

ii. Instantaneous velocity flow maintained higher numerical solution at every nodes compare to transient pressure (Tables 3-7).

iii. The numerical solutions obtained for instantaneous velocity $v(t,z)$ and transient pressure $p(t,z)$ are plotted on 3D plots (Figures 10 to 13) where significant difference are observed.

5.2 Conclusion

We successfully formulate and applied seven steps algorithm for the numerical solutions of system of partial differential equations which occur in fluid dynamics and water flow phenomenon. The algorithm is applied in a discretization way of finite element method. Density of water, diameter and wall thickness of pipe are considered for computational experiment. From the numerical points of view, the algorithm is feasible, efficiency, stable and accurate. We therefore recommend Crank- Nicolson algorithm for solving similar problems in applied sciences, engineering, water transportation and fluid mechanics.

References

[1] Wylie, E. B., and Streeter, V. L. “Fluid Transients in Systems”, Prentice Hall, Englewood Cliffs, New Jersey, USA, 1993.

[2] Sibetheros, I.A., Holley, E.R. and Branski J.M. “Spline Interpolation for waterhammer analysis”. Journal of Hydraulic Engineering 117(10), 1332-1349, 1991.

[3] Twyman, J “Water hammer analysis in a water distribution system”. Ingeniería del Agua 21(2), 87-102, 2017.

[4] Abbott, M.B. and Basco, D.R. “Computational fluid dynamics: an introduction for engineers”. Longman Sc. & Tech., New York, 1989.

[5] CERD. “Lecture note on mathematical model training workshop” at Centre for Energy Research and Development Obafemi Awolowo University, Ile-Ife February 5-8, 2013.

[6] David Ferras, Pedro A. Manso, Anton J. Schleiss and Dídia I. C. Covas “One-dimensional fluid–structure interaction models in pressurized fluid-filled”,2018.

[7] Provenzano, Pablo Gabriel, “Influence of pipe-Diameter on water Hammer phenomena”. Journal of Mechanics Engineering and Automation 370-376, 2015.

[8] Fox, J. A. “Hydraulic Analysis of Unsteady Flow in Pipe Networks”, Macmillan Press Ltd, London, UK; Wiley, New York, USA, 1977.

[9] Twyman, J. “Decoupled hybrid methods for unsteady flow in pipe networks”. Editorial La Cáfila, Valparaíso, 2004.

[10] Záruba, J. “Water Hammer in Pipe-Line Systems (2nd edition)”., Czechoslovak Academy of Sciences, Prague, Czech Republic; Developments in Water Science, 43, Elsevier Science Publishers, Amsterdam, The Netherlands, 1993.

[11] David Ferras, Pedro A. Manso, Anton J. Schleiss and Dídia I. C. Covas “One-Dimensional Fluid–Structure Interaction Models in Pressurized Fluid-Filled Pipes”. Appl. Sci, 8, 1844; 2018.

[12] Crank, J and P. Nicolson, “A practical method for numerical evaluation of solution of partial Differential Equations of the Heat Conduction Type, Proc. Camb. Phil. Soc, 50-67, 1996.

[13] Fadugba S. E, Edogbanya O. H, Zelibe S. C,“Crank Nicolson method for solving parabolic partial differential equations”,International Journal of Applied Mathematics and Modeling IJA2M Vol.1, No. 3, 8-23©Kindi Publications,2013.

[14] Minogue G, N, Oko N, “Numerical solution of parabolic initial – boundary value problem with Crank-Nicolson’s finite difference equations”,IOSR Journal of Mathematics (IOSR-JM), Volume 11, Issue 4 Ver. V (Jul - Aug. 2015), PP 16-19, 2015.

[15] Halil, A, Mehmet, \M, Tülay K, “Application of Crank-Nicolson method to a random component heat equation”,Sigma J Eng & Nat Sci 38 (1), pp475-480, 2020.

[16] Isede H.A, “Several examples of the Crank-Nicolson method for parabolic partial differential equations”. Academia Journal of Scientific Research 1(4) (2013), 063-068, 2013.